Research Article | Vol. 24, No. 20 | 3 Oct 2016 | OPTICS EXPRESS 22741

Optics EXPRESS

C-band swept wavelength erbium-doped fiber laser with a high-Q tunable interior-ridge silicon microring cavity

Nanxi Li,[1,2,*] Erman Timurdogan,[1] Christopher V. Poulton,[1] Matthew Byrd,[1] Emir Salih Magden,[1] Zhan Su,[1] Purnawirman,[1] Gerald Leake,[3] Douglas D. Coolbaugh,[3] Diedrik Vermeulen,[1] and Michael R. Watts[1]

[1]*Research Laboratory of Electronics, Massachusetts Institute of Technology, Cambridge, MA 02139, USA*

[2]*John A. Paulson School of Engineering and Applied Science, Harvard University, Cambridge, MA 02138, USA*

[3]*College of Nanoscale Science and Engineering, University at Albany, Albany, New York 12203, USA*

[*]*nanxili@mit.edu*

Abstract: We demonstrate swept-wavelength operation of an erbium-doped fiber laser using a tunable silicon microring cavity. The microring cavity is designed to have 35 nm free spectral range, a high Q of 1.5×10^5, and low insertion loss of <0.05 dB. The resonance wavelength of the cavity is tuned efficiently (8.1μW/GHz) and rapidly ($\tau_{r,f}$~2.2μs) using an embedded Si heater. The laser achieves single-mode continuous-wave emission over the C-band (1530 nm-to-1560 nm). A mean swept-wavelength rate of 22,600 nm/s or 3106 THz/s is demonstrated within 1532 nm-to-1542 nm wavelength range. Its linewidth is measured to be 16 kHz using loss-compensated circulating delayed self-heterodyne detection.

OCIS codes: (130.3120) Integrated optics devices; (140.3500) Lasers, erbium; (140.3600) Lasers, tunable.

References and links

1. Purnawirman, J. Sun, T. N. Adam, G. Leake, D. Coolbaugh, J. D. Bradley, E. Shah Hosseini, and M. R. Watts, "C- and L-band erbium-doped waveguide lasers with wafer-scale silicon nitride cavities," Opt. Lett. **38**(11), 1760–1762 (2013).
2. E. H. Bernhardi, H. A. G. M. van Wolferen, L. Agazzi, M. R. H. Khan, C. G. H. Roeloffzen, K. Wörhoff, M. Pollnau, and R. M. de Ridder, "Ultra-narrow-linewidth, single-frequency distributed feedback waveguide laser in Al2O3:Er3+ on silicon," Opt. Lett. **35**(14), 2394–2396 (2010).
3. M. Belt and D. J. Blumenthal, "Erbium-doped waveguide DBR and DFB laser arrays integrated within an ultra-low-loss Si3N4 platform," Opt. Express **22**(9), 10655–10660 (2014).
4. Purnawirman, Z. Su, J. D. B. Bradley, E. S. Hosseini, A. Baldycheva, G. Singh, E. S. Magden, T. N. Adam, G. Leake, D. Coolbaugh, and M. R. Watts, "Compact rare-earth-doped microring lasers monolithically integrated on silicon chips," in *CLEO Europe: 2015* (Optical Society of America, 2015), paper CK_12_2.
5. N. Libatique, L. Wang, and R. Jain, "Single-longitudinal-mode tunable WDM-channel-selectable fiber laser," Opt. Express **10**(25), 1503–1507 (2002).
6. D. A. Smith, M. W. Maeda, J. J. Johnson, J. S. Patel, M. A. Saifi, and A. Von Lehman, "Acoustically tuned erbium-doped fiber ring laser," Opt. Lett. **16**(6), 387–389 (1991).
7. F. Xiao, K. Alameh, and T. Lee, "Opto-VLSI-based tunable single-mode fiber laser," Opt. Express **17**(21), 18676–18680 (2009).
8. L. G. Yang, C. H. Yeh, C. Y. Wong, C. W. Chow, F. G. Tseng, and H. K. Tsang, "Stable and wavelength-tunable silicon-micro-ring-resonator based erbium-doped fiber laser," Opt. Express **21**(3), 2869–2874 (2013).
9. Y. Qiu, "Tunable, narrow line-width silicon micro-ring laser source for coherent optical communications," in *CLEO: 2015*, OSA Technical Digest (Optical Society of America, 2015), paper JTh2A.57.
10. F. Aflatouni, B. Abiri, A. Rekhi, and A. Hajimiri, "Nanophotonic coherent imager," Opt. Express **23**(4), 5117–5125 (2015).
11. B. R. Biedermann, W. Wieser, C. M. Eigenwillig, and R. Huber, "Recent developments in Fourier Domain Mode Locked lasers for optical coherence tomograpy: imaging at 1310 nm vs. 1550 nm wavelength," J. Biophotonics **2**, 357–363 (2009).
12. Y. Mao, S. Chang, E. Murdock, and C. Flueraru, "Simultaneous dual-wavelength-band common-path swept-source optical coherence tomography with single polygon mirror scanner," Opt. Lett. **36**(11), 1990–1992 (2011).

#270383 http://dx.doi.org/10.1364/OE.24.022741
Journal © 2016 Received 2 Aug 2016; revised 14 Sep 2016; accepted 15 Sep 2016; published 21 Sep 2016

Optics EXPRESS

13. E. Timurdogan, Z. Su, J. Sun, M. Moresco, G. Leake, D. Coolbaugh, and M. R. Watts, "A high-Q tunable interior-ridge microring filter," in *CLEO: 2014*, OSA Technocal Digest (Optical Society of America, 2014), paper SF2O.3.
14. E. Desurvire, *Erbium-Doped Fiber Amplifiers* (John Wiley and Sons, Inc. Publication, 2002).
15. L. E. Nelson, D. J. Jones, K. Tamura, H. A. Haus, and E. P. Ippen, "Ultrashort-pulse fiber ring lasers," Appl. Phys. B **65**(2), 277–294 (1997).
16. N. Li, J. Xue, C. Ouyang, K. Wu, J. H. Wong, S. Aditya, and P. P. Shum, "Cavity-length optimization for high energy pulse generation in a long cavity passively mode-locked all-fiber ring laser," Appl. Opt. **51**(17), 3726–3730 (2012).
17. Thorlabs. Available: *http://www.thorlabs.de/thorproduct.cfm?partnumber=ER110-4/125*
18. A. E. Siegman, "Ch. 12 Fundamentals of Laser Oscillation," in *LASERS* (University Science Books, 1986).
19. C. Yew Tai, G. J. Cowle, and R. A. Minasian, "Optimization of wavelength tuning of erbium-doped fiber ring lasers," J. Lightwave Technol. **14**(7), 1730–1739 (1996).
20. M. Y. Frankel, R. D. Esman, and J. F. Weller, "Rapid continuous tuning of a single-polarization fiber ring laser," IEEE Photonics Technol. Lett. **6**(5), 591–593 (1994).
21. C. Yew Tai and G. J. Cowle, "Suppression of relaxation oscillations in tunable fiber lasers with a nonlinear amplified loop mirror," IEEE Photonics Technol. Lett. **7**(5), 485–487 (1995).
22. J. W. Dawson, N. Park, and K. J. Vahala, "An improved delayed self-heterodyne interferometer for linewidth measurements," IEEE Photonics Technol. Lett. **4**, 1063–1066 (1992).

1. Introduction

Compared to lasers using a semiconductor gain medium, lasers based on erbium-doped gain medium have a wide bandwidth across the S, C and L bands. Erbium-doped lasers can achieve a narrow linewidth with large side mode suppression ratios (SMSR) due to homogeneously-broadened gain. Since erbium can be co-sputtered with its hosts (e.g. silica, alumina or phosphate glass), integration into a complementary metal-oxide semiconductor (CMOS) compatible platform is straightforward and the low thermo-optic coefficient of the host media enables operation over a wide temperature range. Erbium-doped waveguide lasers with on-chip cavities have been demonstrated with continuous wave lasing in the C and L bands [1–4]. However, the lasers were not actively tuned. Laser wavelength can be tuned by perturbing the cavity: A tunable Bragg grating [5], an acoustic optic modulator [6], or an opto very-large-scale integration (VLSI) processor [7] were used to form tunable lasers. These methods were off-chip and hence not applicable for CMOS integrated platforms. Lasers using erbium doped fiber as gain medium with silicon microdisk cavities have also been demonstrated with passive [8] and active [9] wavelength tunability. However, these demonstrations were not efficient due to losses inside the microdisk cavity. More importantly, the frequency modulated and/or swept-wavelength operation of these lasers using on-chip cavities has not been investigated. Such operation can lead to sources for frequency-modulated continuous-wave laser imaging, light detection and ranging (FMCW-LIDAR) [10] and optical coherence tomography (OCT) at telecom wavelengths [11, 12]. Therefore, a low-loss, high-Q tunable cavity is desired for high swept rate tunable laser sources. Recently, we demonstrated a tunable interior-ridge silicon microring cavity filter with an insertion loss of 0.05 dB and a roughness limited internal Q of 1.5×10^5 [13]. The silicon microring filter had a 3μm radius and a 35 nm free-spectral-range (FSR) that can be continuously and efficiently tuned (8.1 μW/GHz) at high speed (fall time $t_f = 2.6$ μs, rise time $t_r = 1.6$ μs).

Here, we combine the low loss tunable interior-ridge silicon microring cavity with an erbium-doped fiber to form a swept-wavelength laser. A maximum output power of 2.2 mW with a linewidth of 16 ± 1 kHz is measured and the laser is operated with uniform output power over the C-band from 1530 nm to 1560 nm. When the cavity is rapidly tuned, the swept-wavelength laser response is observed at a mean sweep rate of 22,600 nm/s or 3106 THz/s and a peak rate of 91,300 nm/s or 11605 THz/s.

Optics EXPRESS

2. Tunable silicon microring cavity design and characterization

A large uncorrupted FSR was essential for broadband tunability, which required a compact and single mode resonator. For this purpose, we selected an interior ridge silicon resonator, which introduces a hard outer wall. The high index contrast at the outer wall enables tight bend of the waveguide without leaking the mode. Bend induced loss limited internal quality factors (Q) of an interior ridge resonator and conventional ridge bend waveguides are 10^7 and 10^3 respectively for an outer radius of 3.0 μm, shown in Fig. 1(a). The Q is calculated using the complex propagation constant that is simulated with a finite-difference-cylindrical-eigenmode-solver (FDCEM). The radius of an interior ridge resonator can be further reduced to 2.0 μm while keeping a Q about 1.5×10^5, which is the line-edge roughness limited Q in our fabrication process. For tunability of this resonator, an embedded silicon heater is formed within the ridge-etched region, using low and high dose p-type implants. The attachment of a silicon heater to the waveguide core directly heats silicon in a thermally isolated environment (i.e. buried SiO_2), achieving efficient thermal tuning. This is true if the electrodes that pass current through the heater are isolated from the heater. The low resistance narrow silicon tethers are placed for this purpose. The addition of electrodes within the silicon resonator set the minimum outer radius to 3 μm due to fabrication limitations between the contacts. The FSR of this resonator is 35 nm. The position of the doped regions is optimized for minimum absorption due to the embedded heater. The internal Q was simulated using the FDCEM as a function of doping offset, which is the distance between the outer wall and interior doped region. The simulation result is shown in Fig. 1(b). The doping offset that results with an internal Q above 1.5×10^5 is determined to be above 0.4 μm. The resistance of the heater should be reduced to minimize drive voltage, which is required for CMOS compatibility ($P_H = V^2/R$). Our heater resistance is reduced by forming the heater with multiple resistors that are connected in parallel shown in Fig. 1(c). The cavity Q is measured to be 1.5×10^5. The Q measurement and the fabrication of the cavity are described in [13].

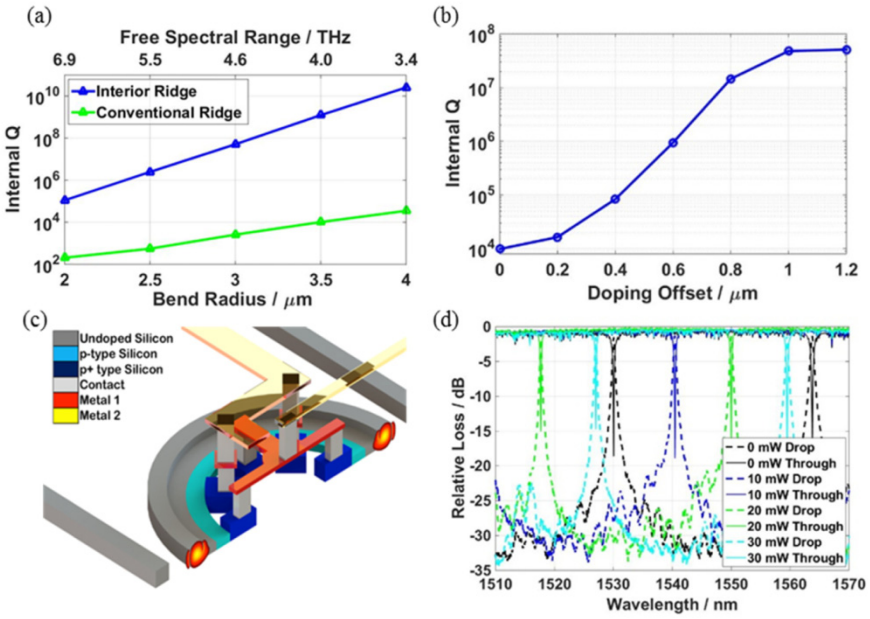

Fig. 1. (a) Quality factor scaling as a function of bend radius for conventional ridge and interior ridge resonators. (b) The simulated quality factor as a function of doping offset under 3 μm bend radius (c) 3D-sketch of the interior-ridge silicon microring cavity. (d) The spectral response of the cavity as a function of heater power.

Optics EXPRESS

For critical coupling and near perfect reflection, the silicon cavity is placed 150 nm away from the bus waveguides. The through and drop ports of the cavity is measured as a function applied heater power, shown in Fig. 1(d). When the heater power of 30 mW is applied, the resonance wavelength of the cavity tuned over the C-band from 1530 nm to 1560 nm, mapped to the gain spectrum of EDF [14].

3. Widely tunable laser design and characterization

Further, the microring filter is used to form a tunable laser within a fiber loop, shown in Fig. 2(a). The loop consists of an erbium doped fiber (EDF), a polarization controller, an output coupler and two wavelength division multiplexers for coupling optical pump in and out of the fiber loop. The fiber loop is supporting a travelling wave, single longitudinal mode, which is commonly used in fiber lasers for ultrashort-pulse generation [15] and observation of solitons [16]. Its unidirectional property is achieved with an isolator. The EDF, with 45 cm length, is single mode (core diameter of 4 μm) and has a doping concentration of 6.6×10^{19} ions/cm^3 that introduces 110 dB/m absorption at 1530 nm [17]. The polarization controller is used to ensure that the light from the fiber is coupled into the TE mode of the microring. A 6.5 μm spot-size lensed fiber is used for coupling optical power to an on-chip inverted Si taper coupler with high efficiency. 10% of the laser power is collected from the output coupler. To measure the loss within the laser system, a 1536 nm laser source is used to probe the laser cavity. The total fiber-to-fiber insertion loss is measured to be around 8.5 dB, which is mainly caused by the coupling loss between the lensed fiber and the on-chip edge-coupler. Based on the loss budget in Fig. 2(b), the total loss in the laser cavity in the operational regime is ~12.45 dB, including 11.6 dB internal loss and 0.85 dB external loss. With a given loss budget, the laser output power can be estimated from the lightly coupled laser oscillator model as shown in Eq. (1) [18]

$$P_{\text{out}} = \delta_e \left(\frac{g}{\delta_e + \delta_o} - 1 \right) P_{\text{sat}} \tag{1}$$

where g is the round trip gain, which has a range from 0 to 7. It is the product of the pump power, which is from 0 up to 460 mW, and the unsaturated gain, which is measured to be 0.015/mW. δ_o and δ_e are internal and external cavity loss, P_{sat} is the saturation power of the EDF gain. Based on the laser loss budget, δ_e is 0.85 dB, corresponding to the loss of the output coupler. δ_o is chosen to be 11.6 dB, corresponding to measured laser cavity internal loss. The internal loss is reduced to 3.6 dB, corresponding to measured internal loss without fiber-to-chip and chip-to-fiber coupling loss, to observe the effects of on-chip gain media. Based on EDF parameters, P_{sat} is calculated to be 2.5 mW. The laser output powers under different internal losses are calculated as a function of pump power, shown in Fig. 2(c).

Optics EXPRESS

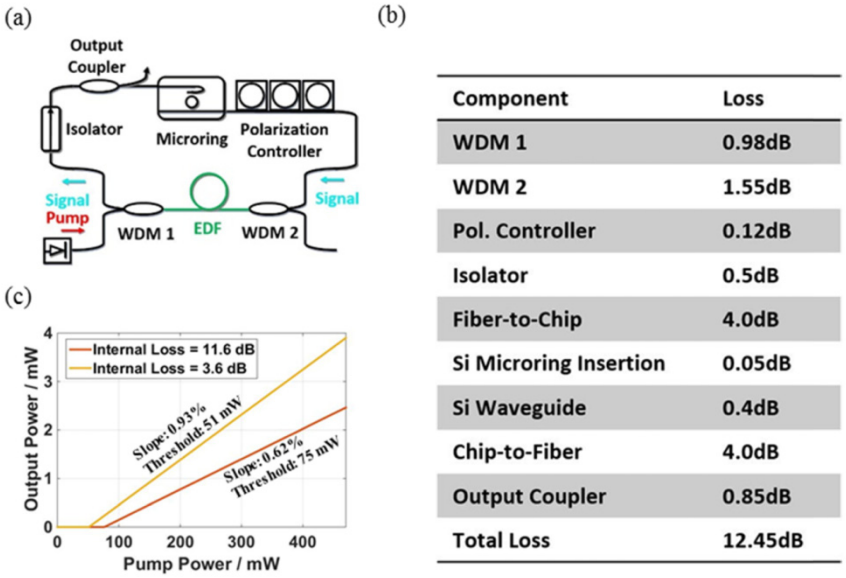

Component	Loss
WDM 1	0.98dB
WDM 2	1.55dB
Pol. Controller	0.12dB
Isolator	0.5dB
Fiber-to-Chip	4.0dB
Si Microring Insertion	0.05dB
Si Waveguide	0.4dB
Chip-to-Fiber	4.0dB
Output Coupler	0.85dB
Total Loss	12.45dB

Fig. 2. (a) The erbium-doped fiber laser with the on-chip cavity setup. (b) The loss budget for the laser cavity. (c) Laser efficiency curve based on lightly coupled laser oscillator model.

When the heater inside the cavity is thermo-optically tuned using a DC voltage, the laser operates with relatively uniform output power (<1.5 dB difference) over the C-band from 1530nm-to-1560nm, shown in Fig. 3(a). Wavelength tuning of up to 30 nm in 5 nm step is observed with corresponding heater powers of up to 30 mW in 5 mW steps. These values correspond to a heater efficiency of 1 mW/nm (~8.1 μW/GHz). The SMSR is found to be larger than 45 dB. The laser efficiency curve at 0 V DC. bias to the tunable microring is shown in Fig. 3(b). The laser output power is observed up to 2.2 mW via an external power splitter. The slope of experimental result matches with the slope of simulation result in Fig. 2(c), for an internal loss of 11.6 dB. The deviation of power measurement points from linear curve can be contributed by the nonlinear absorption within the silicon microring cavity. Due to the intensity enhancement inside the microring cavity, the nonlinear absorption of silicon will ultimately constrain of the maximum output power of our laser device.

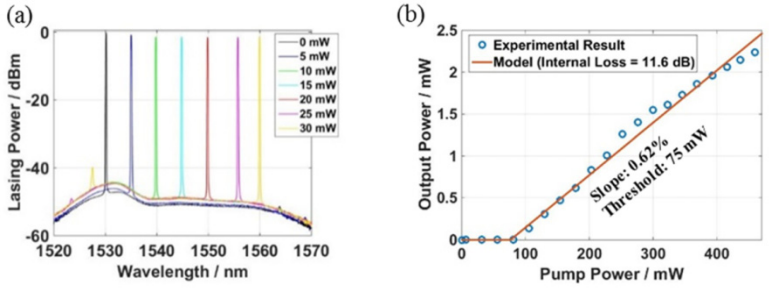

Fig. 3. (a) Laser output wavelengths at different microring heater levels showing operation across C band. (b) Measured lasing efficiency curve with no thermal power applied to the microring.

4. Swept-wavelength or frequency modulated operation

In order to measure the sweep rate of the tunable laser, a separate passive microring resonator is used as a frequency reference. The schematic of the setup is shown in Fig. 4(a). First, electrical modulation is applied on the tunable microring filter within the laser cavity. The

Optics EXPRESS

electrical modulation signal is a sinusoid, with 2.10 V peak to peak and a 2.77 V DC. offset. The frequency is first set to 100 Hz. The output spectrum of the tunable laser is shown in Fig. 4(b) under a maximum hold on an optical spectrum analyzer. It shows that our tunable laser under such modulation spans a 10 nm wide range, from 1532 to 1542 nm. This wavelength range is selected to maintain linearity of the wavelength tuning with a sinusoidal heater voltage. For a wider wavelength range, the drive signal needs to be engineered to maintain linearity. Then the laser output is injected into the passive microring resonator, with 2.1 nm FSR as shown in Fig. 4(c). As the tunable laser wavelength passes the resonant wavelength of reference microring resonator, the output signal recorded by the oscilloscope reveals a dip in transmission, as shown in Fig. 4(d). The 5 ms time span in Figs. 4(d) and 4(e) covers half of the electrical modulation period. Within this time duration, the tunable laser sweeps from 1532 nm to 1542 nm and then goes back to 1532 nm, passing through the resonances of reference microring resonator twice. In Fig. 4(c), the wavelength difference between 1st and 4th resonance is $\Delta\lambda = 6.45$ nm, and in Fig. 4(d) the time difference between 1st and 8th dip is $\Delta t = 4.52$ ms. Therefore, the mean sweeping rate of our tunable laser can be calculated to be $2\Delta\lambda/\Delta t = 2854$ nm/s, corresponding to 362.35 THz/s. Figure 4(e) plots the swept wavelength with respect to time. By taking the maximum slope of the polynomial fitting curve, the peak sweeping rate is calculated to be 4290 nm/s, corresponding to 545.44 THz/s. In order to determine the maximum sweeping rate, the modulation frequency is further increased up to 800 Hz. This value is chosen because nonlinearities are observed above this frequency. The results for this case are shown in Figs. 4(f)-4(g). The mean and peak sweeping rates are measured to be 22,600 nm/s (3061 THz/s) and 91,300 nm/s (11605 THz/s) respectively. The swept-rate is ultimately limited by the relaxation oscillation within the erbium doped fiber [19]. The rate can be increased if the oscillation between switched wavelengths can be controlled with an electrical feedback-loop [20] or a nonlinear loop mirror with a gain equalizing filter [21].

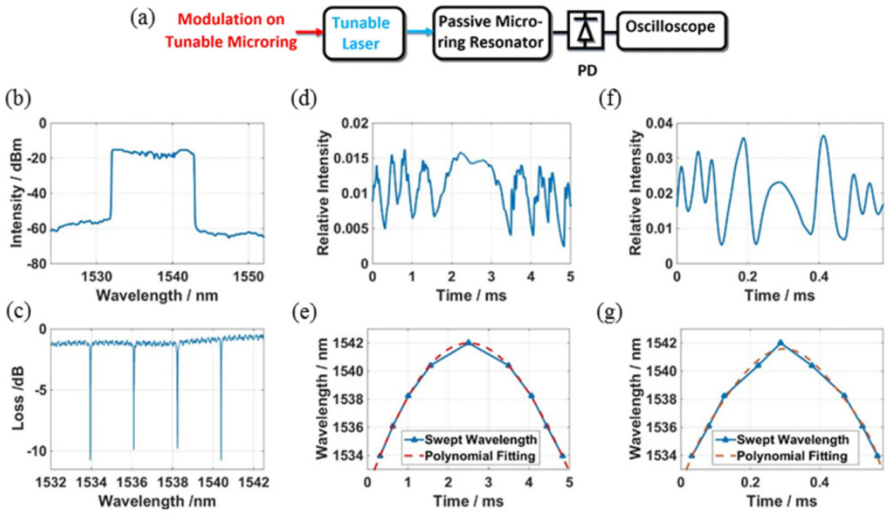

Fig. 4. (a) Sweep rate measurement setup (b) The measured swept-wavelength response with an optical spectrum analyzer using maximum hold setting to show wavelength tuning range. (c) The passive spectrum of the reference SiN resonator with 2.1nm free-spectral-range. (d)/(f) Time domain signal after the microring resonator at 100 Hz and 800 Hz modulation frequency. (e)/(g) Swept wavelength with respect to time at 100 Hz and 800 Hz modulation frequency.

5. Laser linewidth measurement

In order to measure the narrow linewidth (< 1MHz) of the Er tunable laser, the delayed self-heterodyne detection method [22] is used. The setup is shown in Fig. 5(a). The laser signal at

Optics EXPRESS

1530 nm (0 voltage applied to microring) is split into two by the 3dB coupler on the left side. One signal goes through polarization controller 1 (PC 1), and the other signal goes through a delay line. Here the delay line is constructed in a circulating loop as shown in the lower loop of the measurement setup. An acousto-optic modulator (AOM) provides a frequency shift of 44 MHz. Since our Er laser has narrow linewidth, a fiber delay of 35 km is used, and as the circulation number N increases, the total delay length increases. This circulating structure ensures there are higher order harmonics which are incoherent with the signal propagating through PC1. While the circulating number N increases, the SNR in the loop decreases. Hence, an erbium doped fiber amplifier (EDFA) is used to compensate the loss of the circulating loop and maintain the SNR. A tunable filter is tuned to signal wavelength to suppress the amplified spontaneous emission of EDFA. A series of beating signals are detected by an electrical signal analyzer (ESA) and are shown in Fig. 5(b). This spectrum contains harmonics from the 1st to 20th orders. The measured linewidth of each harmonic, as illustrated in Fig. 5(c), has an increasing trend. The linewidth reaches a stable value when the harmonic number is larger than 15. A stable and narrow linewidth of 16 ± 1kHz is observed with no coherence artifacts after a delay length of 350 km (>10th harmonic). The 18th harmonic (f = 18x44 MHz = 792 MHz) electrical response and the Lorentzian fitting are shown in Fig. 5(d). Such a laser linewidth corresponds to a coherence length of 13 km, which is significantly shorter than the total 350 km fiber delay length. This verifies that the delay length used here is long enough to ensure incoherence.

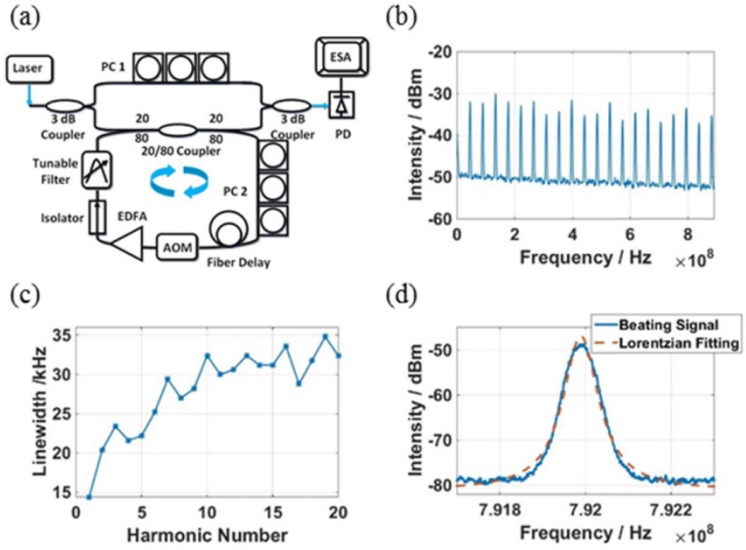

Fig. 5. (a) Linewidth measurement setup: loss-compensated circulating delayed self-heterodyne detection (b) The beating signal of 20 harmonics (c) Linewidth measurement for different harmonics (d) Self-heterodyne spectrum with Lorentzian fitting showing a combined linewidth of 16 kHz.

6. Conclusion

We successfully demonstrated an erbium-doped fiber laser with a tunable interior-ridge Si microring cavity. Laser tunability is achieved by thermally tuning the microring filter. The filter demonstrated has Q factor 1.5×10^5, insertion loss <0.05 dB, and tuning efficiency 8.1 μW/GHz. Continuous wavelength tuning is achieved over a wide wavelength range (C-band) with output powers up to 2.2 mW. The laser with narrow linewidth (16 kHz) and high speed swept-wavelength operation (91,300 nm/s) represents a promising uncooled FMCW-LIDAR or OCT source.

Optics EXPRESS

Funding

Defense Advanced Research Projects Agency (DARPA) E-PHI (grant no. HR0011-12-2-0007) project and DODOS (grant no. HR0011-15-C-0056) project.

Acknowledgment

N. Li acknowledges a fellowship from the Agency of Science, Technology and Research (A*STAR), Singapore.